Diffusion Spectrum Imaging at *7T* for probing Restricted compartment of Textile-based Phantom

Sudhir Kumar Pathak

University of Pittsburgh

Pittsburgh, PA

Introduction

Diffusion processes in biological tissue can be mathematically described using three/two compartments: intra-axonal (restricted compartment) or extra-axonal (hindered compartment) and free water.

Multi-shell or diffusion spectrum imaging-based sampling, varying b-value, diffusion gradient directions, and/or diffusion time is used to model each compartment.

CHARMED, NODDI, and SMT directly estimate diffusivities and volume fractions of each compartment.

Generalized q-sampling imaging, restricted diffusion imaging, generalized diffusion spectrum imaging, and restriction diffusion spectrum imaging estimate the average ensemble propagator (EAP) and derived markers.

Validating these models in biological tissue is challenging due to the complexity of white matter tissue. Idealized, replicable, and scalable phantoms are needed to overcome these challenges and mimic each compartment with known fibers and density patterns.

This study used RDI and GDSI-based reconstruction to quantify restricted, hindered, and free water compartments. Derived markers show significant differences were found between water-filled and unfilled taxons in RDI-based metrics at different length scales (2μ, 4μ, and 6μ) and GDSI-based markers at various length scales (1μ, 2μ, 4μ, 6μ, and 8μ).

Phantom Design

Phantoms are constructed using synthetic fibers with **0.8μ diameter** to mimic the **restricted compartment**-like white-matter tissue. The **hindered compartment** is created by controlling the **density pattern** of these fibers in a cube.

Two variants of phantoms are manufactured that are suitable for scanning on a **7T bruker animal scanner**; each phantom contains a similar cube with taxons with a **0.8μ diameter**

o Filled with pure water

o filled with dissolvable copolyester

The first variant mimics restricted (inside fiber) and hindered compartments (outside fiber), and the second mimics only hindered compartments.

Both variants of the phantom are created by 3D printing a cubic shell that is hollow inside to hold the filled and non-filled versions of taxons.

Taxsons are created using nylon and can contain dissolvable copolyester or water. Water filling for the second variant requires four weeks of treatment; see for detail. Both phantoms are further put inside a cylinder filled with pure water.
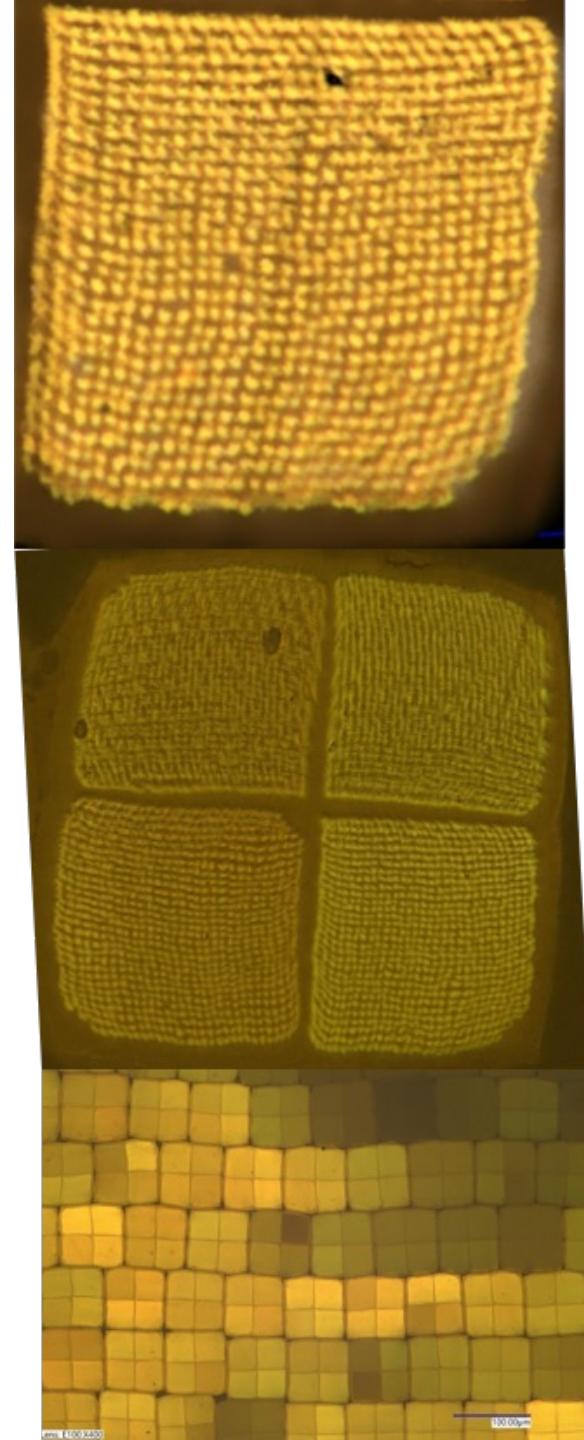
Data Acquisition and Methods

MRI Scanning

Both phantoms were scanned on a 7T Bruker animal scanner with $b_{max}=5000 \ s/mm^2$ with *107 non b=0* gradient directions *and 15 b=0 s/mm²* (Total *122 dwis*). Stimulated echo is used with the BCC sampling scheme of q-space with FoV *3.0x3.0cm*: voxel size: *0.117x0.117x0.5mm³* with 20 axial slices, *TE=12.31ms, TR=5000ms, δ=2ms, and Δ=80ms*.

Reconstruction

Generalized Diffusion Spectrum Imaging

- GDSI is used to reconstruct EAPs using an in-house PyTorch-based Python program that takes 12 hours of computation on NVIDIA GPU 2080Ti.
- Recovered EAPs for each voxel are sampled in 1024 angular directions and 100-sample radially between 0.0 and 1.0 (1.0 being the mean displacement distance of free water).
- Five scalar metrics are estimated as a probability at displacement r averaged across all directions (*r=1,2,4,6,8μ*).
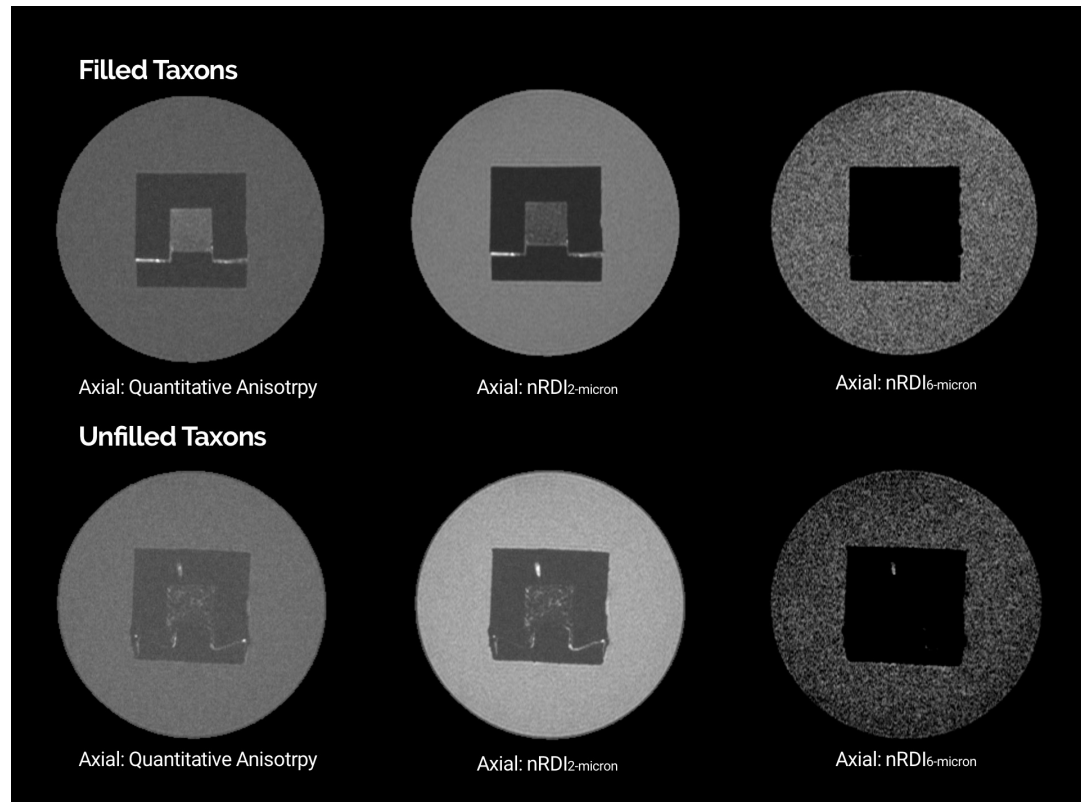
Restricted Spectrum Imaging

- Using DSI Studio, Restricted Spectrum Imaging estimates non-restricted diffusion imaging (*nRDI*) for three length scales, *L=2,4,6μ*.
- In addition, a *quantitative anisotropy (QA)* map is also estimated using GQI reconstruction algorithms.
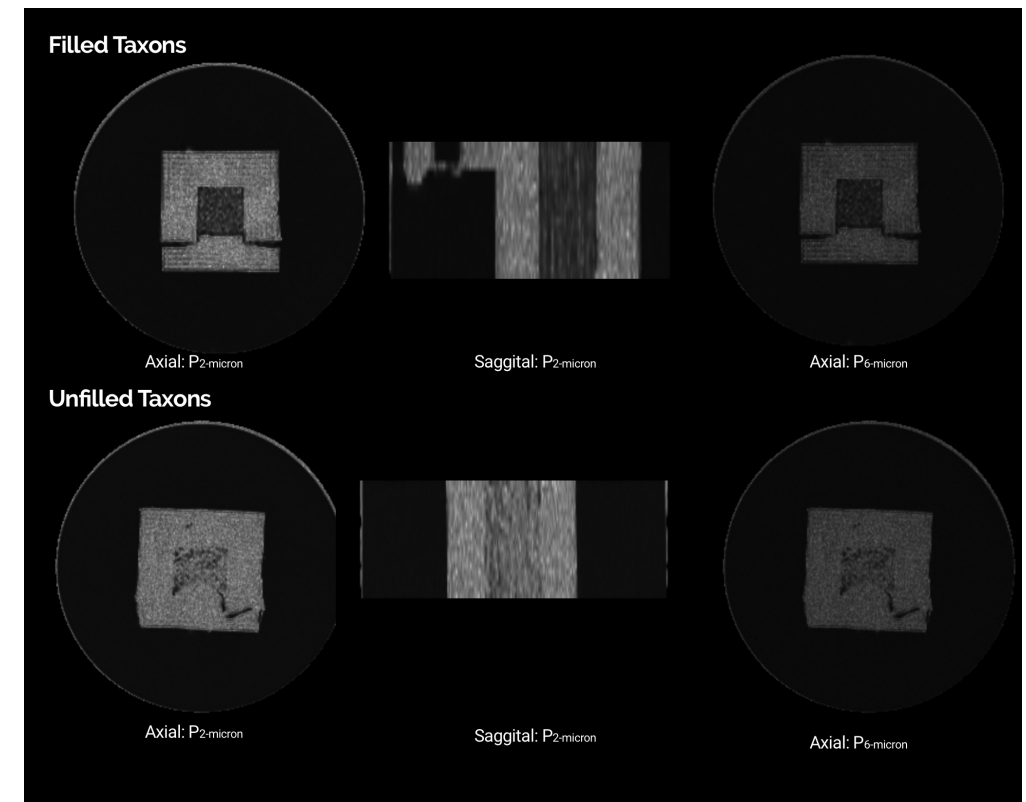
Statistical Analysis

- All derived metrics from GDSI ($P_{1\mu}$, $P_{2\mu}$, $P_{4\mu}$, $P_{6\mu}$, $P_{8\mu}$) and GQI/RDI (QA, $nRDI_{2\mu}$, $nRDI_{4\mu}$, $nRDI_{6\mu}$) are further used for the statistical test for three ROIs (Pure water: **Pink**, Outer 3D material: **Orange**, and water-filled taxons: **Blue**).
- Statistical tests and box/violin plots are created using R's ggplot package.
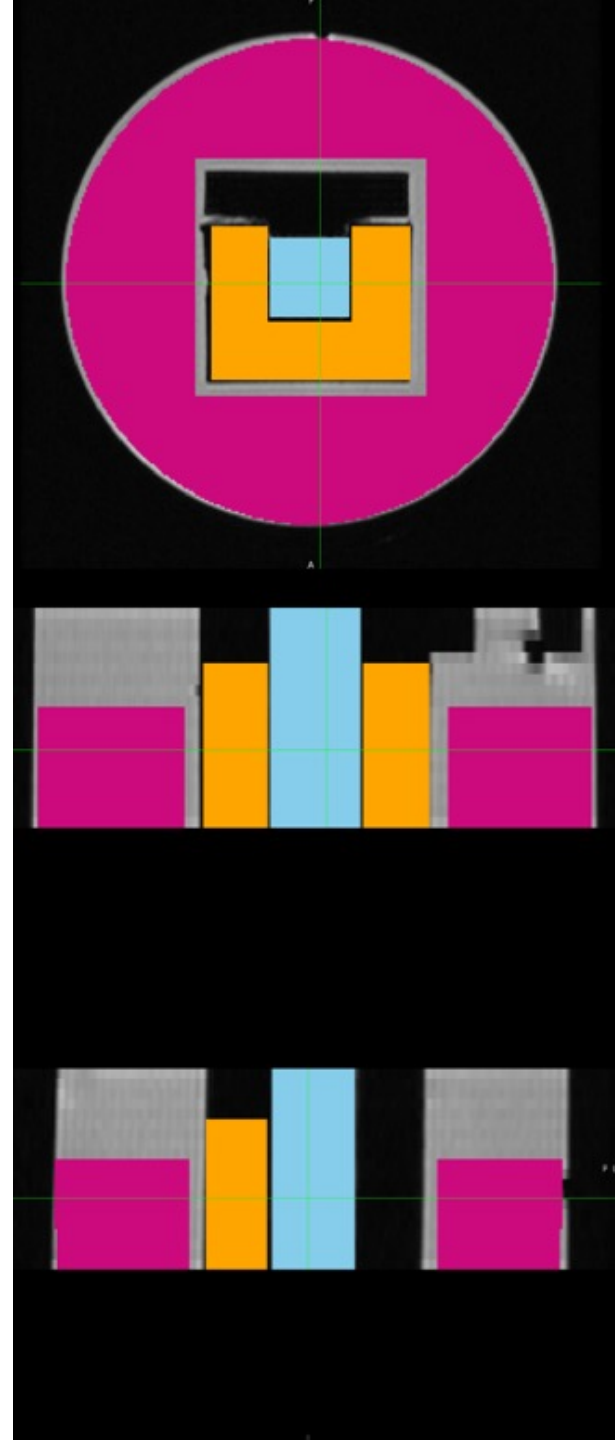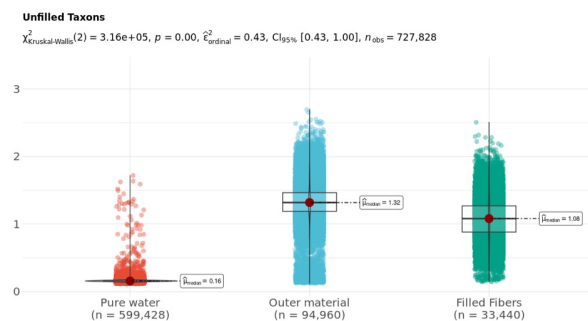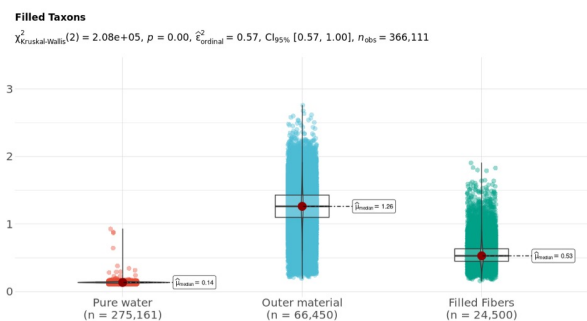
Results

Generalized Diffusion Spectrum Imaging

Restricted Spectrum Imaging

Axial and transversal view of biomarkers estimated using 1) **GDSI** with five different length scales for filled and non-filled taxons. Sagittal views show a stripped-like pattern for the filled taxons compared to non-filled taxons, indicating the restricted compartment's length scale. 2) **RDI-derived** quantitative anisotropy and non-restricted diffusion map at 2μ and 6μ-length scales. At 6μ, the restricted compartment disappeared. On the other hand, QA and $nRDI_{2\mu}$ show uniform values within the cube with water-filled taxons.
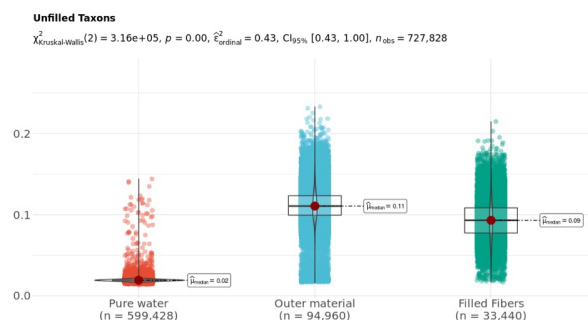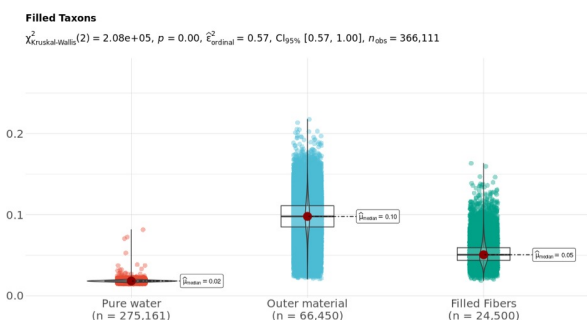
Results

Restricted Spectrum Imaging

Quantitative Anisotropy

Normalized RDI 2µ

Generalized Q-Sampling Imaging (GQI) based scalar metric, Yeh et al 2010

Normalized RDI 6µ

Generalized Q-Sampling Imaging (GQI) based scalar metric, Yeh et al 2010

Generalized Diffusion Spectrum Imaging

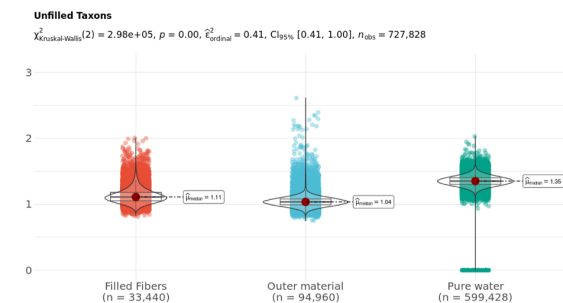Probability at 2µ averaged across all directions
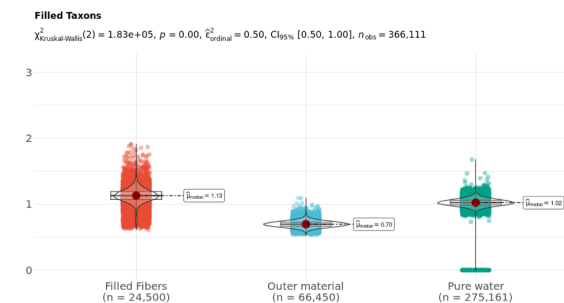

Probability at 6µ averaged across all directions

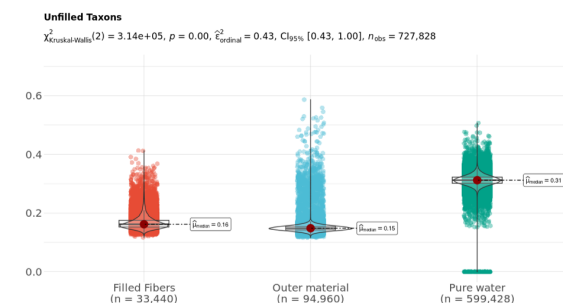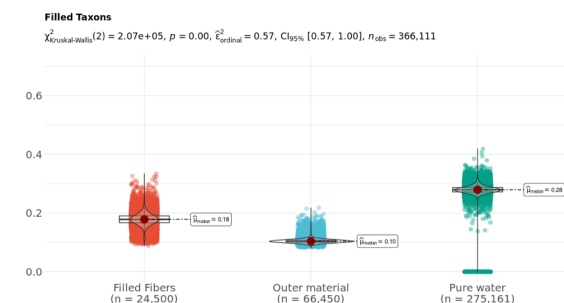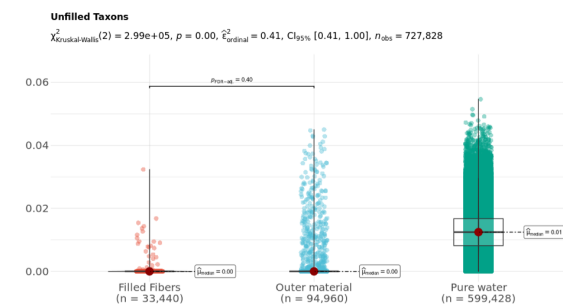Generalized Diffusion Spectrum Imaging based scalar metric, Tian et al 2019
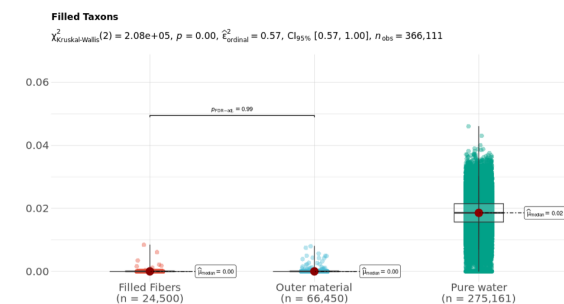
The statistical difference between 3-ROIs for each *GDSI*-derived and each *nRDI* and *QA* metric. Each metric shows a significant difference between pure water and restricted compartment, and this difference decreases at a larger length scale (for *RDI* difference disappears at *6µ*).

Conclusions

We proposed a design of diffusion-MRI phantom to probe restricted compartments at different diffusion length scales and suitable for a 7T scanner for a high spatial-resolution scan.

DSI-based acquisition/reconstruction methods can quantify restricted and hindered compartments.

Phantom provides an idealized bio-mimicking tissue structure with known diameters suitable for validation of other diffusion methods.

Future studies include calibration across scans and creating restricted compartments with multiple diameters.

References

Yeh, F. C., Wedeen, V. J., & Tseng, W. Y. I. (2010). Generalized q-sampling imaging. IEEE transactions on medical imaging, 29(9), 1626-1635.

Yeh, F. C., Liu, L., Hitchens, T. K., & Wu, Y. L. (2017). Mapping immune cell infiltration using restricted diffusion MRI. Magnetic resonance in medicine, 77(2), 603-612.

Tian, Q., Yang, G., Leuze, C., Rokem, A., Edlow, B. L., & McNab, J. A. (2019). Generalized diffusion spectrum magnetic resonance imaging (GDSI) for model-free reconstruction of the ensemble average propagator. NeuroImage, 189, 497-515.

Chiang, W. Y., Wedeen, V. J., Kuo, L. W., Perng, M. H., & Tseng, W. Y. (2006). Diffusion spectrum imaging using body-center-cubic sampling scheme. In Proc. 14th Annu. Meeting ISMRM (p. 1041).

Kaden E, Kelm ND, Carson RP, Does MD, and Alexander DC: Multi-compartment microscopic diffusion imaging. NeuroImage, vol. 139, pp. 346–359, 2016

Zhang, Hui, et al. "NODDI: practical in vivo neurite orientation dispersion and density imaging of the human brain." Neuroimage 61.4 (2012): 1000-1016

Assaf, Yaniv, and Peter J. Basser. "Composite hindered and restricted model of diffusion (CHARMED) MR imaging of the human brain." Neuroimage 27.1 (2005): 48-58

Li, Hua, et al. "Linking spherical mean diffusion weighted signal with intra-axonal volume fraction." Magnetic resonance imaging 57 (2019): 75-82.

Jelescu, I. O., & Budde, M. D. (2017). Design and validation of diffusion MRI models of white matter. Frontiers in physics, 5, 61.

Nilsson, M., van Westen, D., Ståhlberg, F., Sundgren, P. C., & Lätt, J. (2013). The role of tissue microstructure and water exchange in biophysical modelling of diffusion in white matter. Magnetic Resonance Materials in Physics, Biology and Medicine, 26(4), 345-370.

Huang, S. Y., Witzel, T., Keil, B., Scholz, A., Davids, M., Dietz, P., ... & Rosen, B. R. (2021). Connectome 2.0: Developing the next-generation ultra-high gradient strength human MRI scanner for bridging studies of the micro-, meso-and macro-connectome. NeuroImage, 243, 118530.

Fan, Q., Nummenmaa, A., Wichtmann, B., Witzel, T., Mekkaoui, C., Schneider, W., ... & Huang, S. Y. (2018). Validation of diffusion MRI estimates of compartment size and volume fraction in a biomimetic brain phantom using a human MRI scanner with 300 mT/m maximum gradient strength. Neuroimage, 182, 469-478.

Zuccolotto, Anthony P., et al. "Mri phantom including hollow fluid filled tubular textiles for calibrated anisotropic imaging." U.S. Patent Application No. 16/859,444.

Wedeen, V. J., Hagmann, P., Tseng, W. Y. I., Reese, T. G., & Weisskoff, R. M. (2005). Mapping complex tissue architecture with diffusion spectrum magnetic resonance imaging. Magnetic resonance in medicine, 54(6), 1377-1386.

Jeurissen, B., Tournier, J. D., Dhollander, T., Connelly, A., & Sijbers, J. (2014). Multi-tissue constrained spherical deconvolution for improved analysis of multi-shell diffusion MRI data. NeuroImage, 103, 411-426.

White, N. S., Leergaard, T. B., D'Arceuil, H., Bjaalie, J. G., & Dale, A. M. (2013). Probing tissue microstructure with restriction spectrum imaging: histological and theoretical validation. Human brain mapping, 34(2), 327-346.